

Molecular mechanics of Ag nanowire transfer process subjected to contact loadings by PDMS substrate

Minseok Kang^{a,b}, Hyunkoo Lee^{a,b}, Sukjoon Hong^{a,b,*}, Joonmyung Choi^{a,b,*}

^aDepartment of Mechanical Design Engineering, Hanyang University, 222 Wangsimni-ro
Seongdong-gu, Seoul 04763, Korea

^bDepartment of Mechanical Engineering, BK21 FOUR ERICA-ACE Center
Hanyang University, 55 Hanyangdaehak-ro, Sangnok-gu Ansan 15588, Republic of Korea

* Corresponding author: Prof. Sukjoon Hong
Tel.: +82-31-400-4719
E-mail address: sukjoonhong@hanyang.ac.kr

* Corresponding author: Prof. Joonmyung Choi
Tel.: +82-31-400-5243
E-mail address: joonchoi@hanyang.ac.kr

Supplementary Text 1: Phase transformation of AgNW under uniaxial loading

Uniaxial tensile loading simulations were conducted for the modelled AgNWs with diameters ranging from 2.80 nm to 6.53 nm. All AgNWs had the same lengths (22.35 nm), and the periodic boundary condition was applied in the longitudinal (z) direction. Each model was equilibrated under the NVT ensemble at 300 K for 500 ps with the timestep of 1 fs. Subsequently, the modelled unit cell was deformed in the longitudinal direction at 300 K at a strain rate of $5 \times 10^7/s$ until the maximum strain reached 0.1. **Fig. S1** shows the stress–strain curves of the modelled AgNWs considered in this study. Their Young’s modulus values are 110.7, 108.3, 106.2, and 102.0 GPa in increasing order of the diameter. In addition, it is clearly observed that the yield strength (σ_Y) decreases from 4.15 GPa to 3.71 GPa as the AgNW diameter increases. The yield strain (ϵ_Y) was calculated as approximately 5.7%, irrespective of the diameter condition. It is worth to note that the results are very close to those ($\sigma_Y = 3.80$ GPa and $\epsilon_Y = 0.06$ for AgNWs with 10 nm diameter) obtained by Liang et al.,¹ verifying the parameters of the force field and other modelling factors used in the current study. **Fig. S2** shows the surface nucleation of the stacking fault decahedron (SFD). The stress of the AgNW first increases linearly with the tensile strain in the z-direction and subsequently shows abrupt load drop at first yielding and at maximum strength. A Shockley partial dislocation nucleates at an $\{100\}$ free surface between the adjacent twin boundaries at this point. As the tensile deformation continues to progress, five stacking fault areas are generated on both sides and another dislocation occurs at the adjacent $\{100\}$ free surface. The results correctly reproduce the previous study done by Filleter et al.,² which verifies the validity of the present AgNW model.

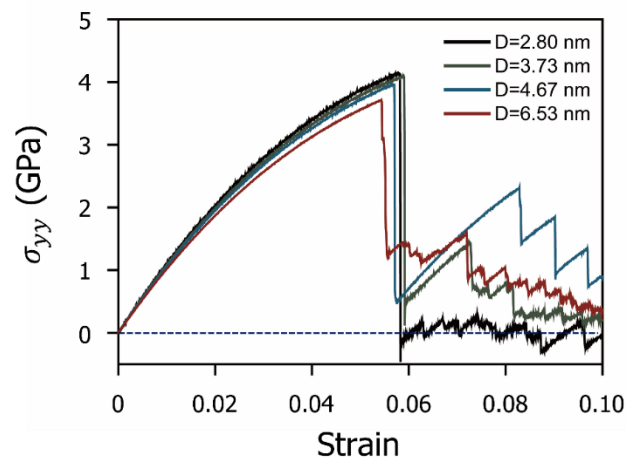


Fig. S1. Stress–strain curves of modelled AgNWs under uniaxial tensile loading.

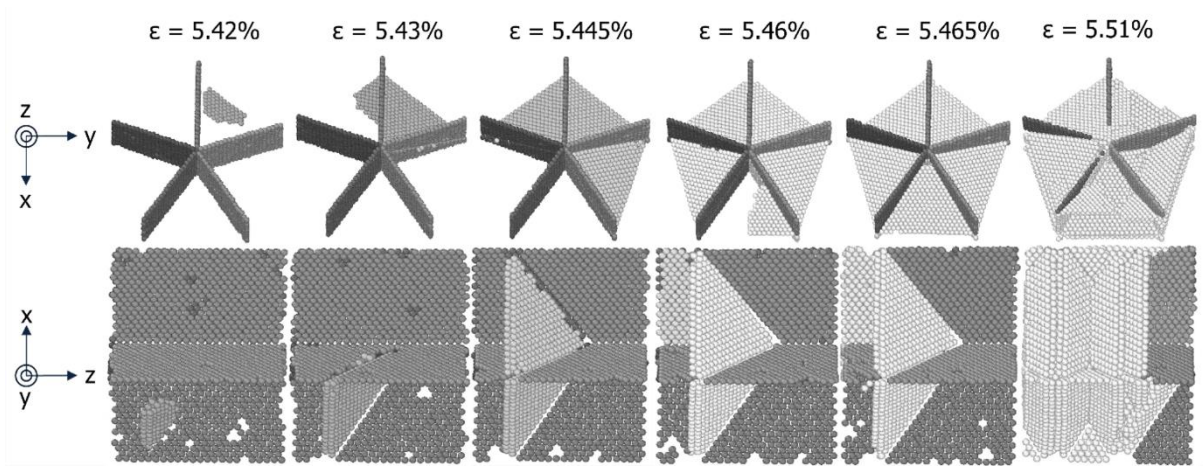


Fig. S2 Formation of SFD in AgNW during uniaxial loading.

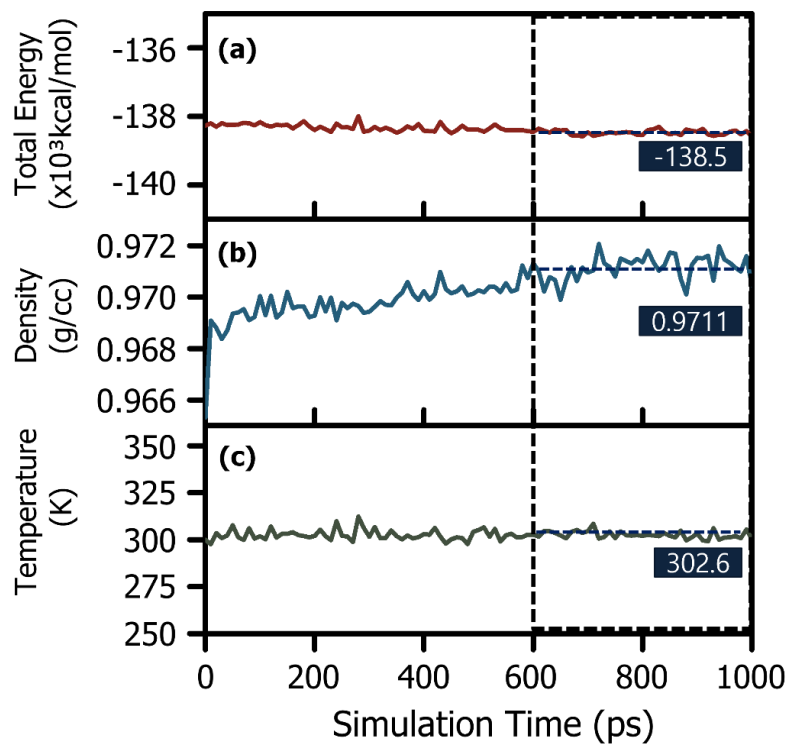


Fig. S3 Variations in (a) total energy, (b) density, and (c) temperature during NPT ensemble of modelled PDMS unit cell.

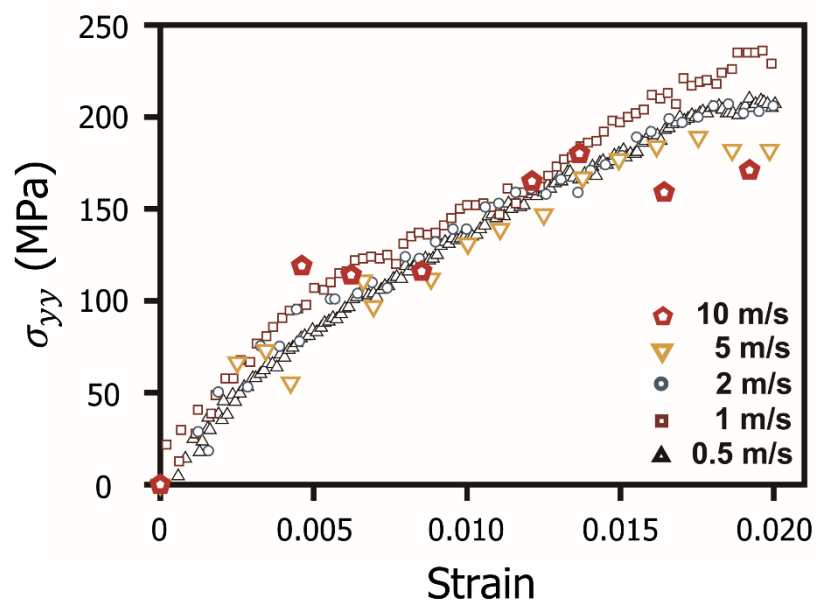


Fig. S4. Convergence of mechanical response characteristics of AgNWs under different pull-out speeds of PDMS substrate. AgNW with diameter of 4.67 nm and aspect ratio of 4.78 is considered as representative model. Stress curves present similar profiles regardless of pull-out speed, indicating that simulation condition used in this study (1 m/s) is valid for evaluating static mechanical properties of AgNWs.

Table S1. Force field parameters between Ag and PDMS constituent atoms used in this study.

| Force field name | Type | r (Å) | ϵ (kcal/mol) |
|------------------|-----------------------------|--------|-----------------------|
| Ag | Silver metal | 3.0222 | 4.1002 |
| osi | Siloxane oxygen | 3.35 | 0.24 |
| sio | Siloxane silicon | 4.284 | 0.07 |
| c3 | Carbon with three hydrogens | 4.01 | 0.054 |
| hc | Hydrogen bonded to carbon | 2.995 | 0.02 |

Supplementary Text 2: Using EAM and PCFF potential parameters together

In this study, both the EAM and PCFF potentials were used to describe the combined AgNW–PDMS substrate system. The use of the EAM potential was limited to the inner region of the AgNWs, and thus, all non-covalent bonding forces formed by the components of PDMS and Ag were calculated using the PCFF potential parameters. Specifically, the non-bonding interaction between PDMS and the AgNWs depended entirely on the PCFF potential parameters. Such a combination is essential in this study because an integrated force field based on the PCFF cannot properly analyse the internal phase transformation of the AgNWs caused by a large deformation. Note that studies on polymer–metal interfaces in which with the EAM is limited to the atoms in the inner region of the metals are also found elsewhere^{S3,S4}.

Moreover, using the PCFF has not only yielded inter- and intramolecular parameters of polymers by experiments and ab initio studies but has also proven to be applicable to various heterogeneous systems, such as polymer–metal^{S5} and polymer–ceramic^{S6} composites. Therefore, interfacial analysis studies between Ag nanosystems and polymeric materials based on the PCFF^{S5,S7,S8} can be easily found. All the above studies particularly focussed on the analysis of the interfacial properties and mechanical roles between two materials and showed that the PCFF reproduces rigorous observations such as experiments and first-principles calculations very well. Based on the reported results, in this study, the non-bonding energy was calculated using the 9–6 Lennard–Jones potential with the sixth-power mixing law without additional parameter modifications related to Ag atoms.

Supplementary Text 3: Delamination simulations at 0.1 K temperature

As mentioned in the main text, mechanical tests in which AgNWs and PDMS substrates were in contact and separated by forced displacements were simulated in a cryogenic environment of 0.1 K. This was done to eliminate the effect of the undesired thermal energy on the virial stress in the processes involving forced restraint and displacement conditions. Both the EAM³⁷ and PCFF³⁸ potentials used in this study have been aimed at quantitatively predicting mechanical properties (e.g., elastic constants) at 300 K when describing solid materials. Therefore, in the absence of rate dependence, such as viscoelastic and thermoelastic properties, the mechanics of materials at 300 K agrees best with MD simulation results considering the potential energy alone.

In this study, room-temperature conditions were considered in the modelling of the stabilized structure of each material, whereas the evaluation of the mechanical properties of the all-atom system based on the virial stress was conducted in a cryogenic environment. This approach has the following two advantages in terms of the simulation methodology. First, it can effectively exclude the aggregation behaviour of PDMS molecules on the AgNWs, which originates from thermal effects. Second, the difference between the potential energies in the constrained and unconstrained regions is sufficiently small only in a cryogenic environment. If the vibrational energy resulting from a finite temperature is employed, the energy distortion of the atoms in the immediate vicinity of the boundary condition will significantly intensify. This is an artefact to avoid in a mechanical test environment. Therefore, to evaluate the mechanical behaviour of the all-atom system using the virial stress calculation formula in Eq. (4), completely excluding the disturbance of the potential energy due to the thermal effect is necessary.

Supporting Reference

1. T. Liang, D. Zhou, Z. Wu, P. Shi and X. Chen, *Nanoscale*, 2018, **10**, 20565-20577.
2. T. Filleter, S. Ryu, K. Kang, J. Yin, R. A. Bernal, K. Sohn, S. Li, J. Huang, W. Cai and H. D. Espinosa, *Small*, 2012, **8**, 2986-2993.
3. M.A.N. Dewapriya and R.E. Miller, *Comput. Mater. Sci.*, 2020, **184**, 109951.
4. M.A.N. Dewapriya and R.E. Miller, *Comput. Mater. Sci.*, 2021, **195**, 110504.
5. S.-P. Ju, H.-Y. Chen and C.-W. Shih, *J. Nanopart. Res.*, 2018, **20**, 1.
6. S. Yu, S. Yang and M. Cho, *Polymer*, 2009, **50**, 945-952.
7. C.-H. Su, H.-L. Chen, S.-P. Ju, H.-Y. Chen, C.-W. Shih, C.-T. Pan and T.-D. You, *Sci. Rep.*, 2020, **10**, 7600.
8. K. Mirabbaszadeh and E. Zaminpayma, *Appl. Surf. Sci.*, 2012, **261**, 242-246.
9. S. M. Foiles, M. I. Baskes and M. S. Daw, *Phys. Rev. B*, 1986, **33**, 7983-7911.
10. H. Sun, *J. Comput. Chem.*, 1994, **15**, 752-768.